

NMR relaxation time around a vortex in stripe superconductors

M. Takigawa, M. Ichioka and K. Machida

Department of Physics, Okayama University, Okayama 700-8530, Japan

(dated: April 14, 2024)

Site-dependent NMR relaxation time $T_1(r)$ is calculated in the vortex state using the Bogoliubov-de Gennes theory, taking account of possible "field-induced stripe" states in which the magnetism arises locally around a vortex core in d-wave superconductivity. The recently observed huge enhancement $T_1^{-1}(r)$ below T_c at a core site in $Tl_2Ba_2CuO_6$ is explained. The field-induced stripe picture explains consistently other relevant STM and neutron experiments.

PACS numbers: 76.60.Pc, 74.60.Ec, 74.25.Jb

Much attention has been focused on microscopic electronic structure, or low-lying excitation spectrum around a vortex core in a superconductor, particularly in the high T_c cuprate superconductor, whose pairing mechanism is still not known. It is expected that the vortex core might be a useful window through which we can probe the ground state in the "normal phase" by removing superconductivity.

Recently, keen interest is stimulated by a series of remarkable experiments: Neutron scattering experiments observe an enhancement of the incommensurate magnetic satellite peaks by applying magnetic fields [1, 2, 3]. The checkerboard pattern of the local density of states (LDOS) in $Bi_2Sr_2CaCu_2O_{8+x}$, or the so-called "halo" is found around a vortex site by scanning tunneling microscopy (STM) experiments by Ho man et al. [4]. Vortex-imaging NMR experiments detect anomalous relaxation time T_1 around a vortex core site in $YBa_2Cu_3O_7$ [5] and $YBa_2Cu_4O_8$ [6]. The set of these experiments collectively point to a notion that incipient spin density wave and/or charge density wave, namely, stripe states in a broad sense are induced around a vortex core by applying a moderate magnetic field.

In d-wave pairing, which is now fairly well established for high T_c cuprate superconductors, the low-lying vortex core excitations are expected to have a finite density of states (DOS) exactly at the Fermi level. Thus the core should be filled up by these quasiparticles and tunneling conductance as a function of the bias voltage should exhibit a zero-energy peak (ZEP) structure at a core. However, the existing STM results [7] so far fail to detect this ZEP, instead they see the empty core, namely there is not any clear structure in the tunneling conductance at a core site. This disparity between the theoretical prediction and experimental facts is rather serious, because in a conventional superconductor such as $2H-NbSe_2$ the observed quasiparticle spectra by Hess et al. [8] are almost perfectly understood theoretically in terms of the bound state trajectories [9]. The situation becomes more serious since the vortex imaging NMR experiments done by Mitrovic, et al. [5] and Kakuyanagi, et al. [6] found that the site-dependent T_1 becomes longer at the vortex core, after being shorter with approaching towards the vortex. It is contradicted with existence of the ZEP of the LDOS, which should lead to the shortest T_1 at the core.

This suggests absence of the ZEP associated with d-wave vortex, being rather consistent with the STM [7].

The emerging notion of the field induced stripe matches with the above neutron experiments because the four site charge modulation corresponding to the STM observation [4] is accompanied by the eight site spin density wave, or stripe, seen as the incommensurate satellites. The applied field with a mere few Tesla enhances those satellite intensities and the estimated induced moment is roughly proportional to H [1].

Prior to the present work, there have been several theoretical attempts to explain some of these facts, notably the STM experiments under H [10, 11, 12, 13, 14, 15, 16, 17] and without H [18, 19]. These theories are based on the field induced incipient spin and/or charge density orders, giving an explanation of the STM observation of four-site periodic LDOS modulation.

Quite recently, two new NMR imaging experiments [20, 21] on the T -dependence of T_1 are reported: Kakuyanagi, et al. [20] show in $Tl_2Ba_2CuO_6$ that as lowering T , $1/T_1$ at a core site increases divergently towards a temperature T_M below T_c and then decreases at lower T . This is contrasted with $1/T_1$ at other sites which exhibit a monotonic decrease below T_c . This result suggests that below T_M the magnetism appears locally exclusively at a vortex core site and other sites stay in the normally expected d-wave state. Mitrovic, et al. [21] observe a similar divergent behavior in $1/T_1$ of $YBa_2Cu_3O_7$ for the core site where the crossover temperature T_M is quite low and $1/T_1$ for the sites outside the core shows a constant at low T . The implication of these experiments is two-fold: The missing ZEP in d-wave vortex core must be present in the limited T and H region. Below T_M the locally field induced stripe must exist, which is to remove the ZEP, giving rise to a suppression of T_1^{-1} at lower T .

The purpose of this study is to demonstrate that the field induced stripe picture explains these experimental facts in a coherent way. This is done by explicitly calculating the site-dependent T_1 , based on the Bogoliubov-de Gennes (BdG) equation for d-wave superconductors. Our calculation shows that the vortex imaging NMR [22, 23, 24] yields a wealth of information on d-wave superconductors under H .

We begin with the standard Hubbard model on a two-dimensional square lattice, and introduce the mean field

$n_{i\uparrow} = \hat{n}_{i\uparrow}^y$, $a_{i\uparrow}$ at the i -site, where i is a spin index and $i = (i_x, i_y)$. We assume a pairing interaction V between nearest-neighbor (NN) sites. This type of pairing interaction gives d-wave superconductivity [22, 23]. Thus, the mean-field Hamiltonian under H is given by

$$H = \sum_{i,j} t_{ij} a_{i\uparrow}^\dagger a_{j\uparrow} + U \sum_i n_{i\uparrow} a_{i\uparrow}^\dagger a_{i\uparrow} + V \sum_{\langle i,j \rangle} (a_{i\uparrow}^\dagger a_{j\uparrow} + a_{i\downarrow}^\dagger a_{j\downarrow} + \text{h.c.}) \quad (1)$$

where $a_{i\uparrow}^\dagger$ ($a_{i\uparrow}$) is a creation (annihilation) operator, and $i + \hat{e}$ represents the NN site ($\hat{e} = \hat{x}; \hat{y}$). The transfer integral is expressed as

$$t_{ij} = t_{ij} \exp \left[i \int_0^{r_j} A(r) dr \right]; \quad (2)$$

with the vector potential $A(r) = \frac{1}{2} \nabla \times \mathbf{r}$ in the symmetric gauge, and the flux quantum ϕ_0 . For the NN pairs (i, j) , $t_{ij} = t$. For the next-NN pairs situated on a diagonal position on the square lattice, $t_{ij} = t^0$. For the third-NN pairs, which are situated along the NN bond direction, $t_{ij} = t^0$. To reproduce the Fermi surface topology of cuprates, we set $t^0 = 0.12t$ and $t^0 = 0.08t$ [25]. We consider the pairing interaction $V = 2.0t$. The essential results of this paper do not significantly depend on the choice of these parameter values.

In terms of the eigen-energy E and the wave functions $u(r_i)$, $v(r_i)$ at the i -site, the BdG equation is given by

$$\begin{pmatrix} K_{ij} & D_{ij} \\ D_{ij}^\dagger & K_{ij} \end{pmatrix} \begin{pmatrix} u(r_j) \\ v(r_j) \end{pmatrix} = E \begin{pmatrix} u(r_i) \\ v(r_i) \end{pmatrix}; \quad (3)$$

where $K_{ij} = t_{ij} + i_{ij}(U n_{i\uparrow})$, $D_{ij} = V e^{-i_{ij}} \langle a_{i\uparrow}^\dagger a_{j\uparrow} \rangle$ and i is an index of the eigenstate [22, 23]. The self-consistent condition for the pair potential and the number density is given by $i_{ij} = \langle a_{i\uparrow}^\dagger a_{j\uparrow} \rangle = \int \frac{dE}{2\pi} u(r_i) v(r_j) f(E)$, $n_{i\uparrow} = \langle a_{i\uparrow}^\dagger a_{i\uparrow} \rangle = \int \frac{dE}{2\pi} |u(r_i)|^2 f(E)$, $n_{i\downarrow} = \langle a_{i\downarrow}^\dagger a_{i\downarrow} \rangle = \int \frac{dE}{2\pi} |v(r_i)|^2 f(E)$. The charge density $n_i = n_{i\uparrow} + n_{i\downarrow}$, the spin density $S_{z,i} = \frac{1}{2}(n_{i\uparrow} - n_{i\downarrow})$ and the staggered magnetization $M_i = S_{z,i} (1)^{i_x + i_y}$. The d-wave order parameter at site i is $\Delta_i = (a_{i\uparrow}^\dagger - a_{i\downarrow}^\dagger) / \sqrt{2}$ with

$$e_{ij} = \int_0^{r_{i+j}} A(r) dr;$$

where $i_{i+j} = \langle a_{i+j}^\dagger a_i \rangle = \langle a_{i+j}^\dagger a_i \rangle$.

We typically consider the case of a unit cell with 24×24 sites, where two vortices are accommodated. The spatially averaged hole density is set to $n_h = 1 - \bar{n}_i = \frac{1}{8}$ by tuning the chemical potential μ . By introducing the quasimomentum of the magnetic Bloch state, we obtain the wave function under the periodic boundary condition whose region covers many unit cells.

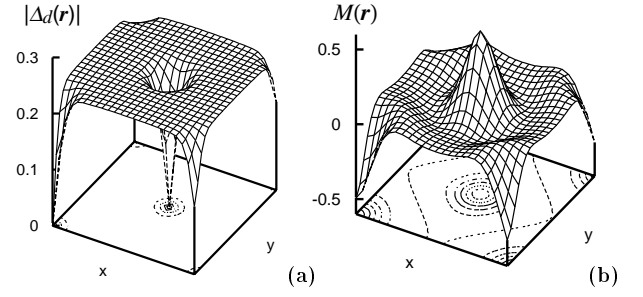


FIG. 1: Spatial structures of the d-wave order parameter $\Delta_d(r)$ and the induced staggered moment $M(r)$. At the vortex core site V , $\Delta_d(r) = 0$. The unit cell size is 24×24 . $U/t = 3.0$. $T/t = 0.01$.

We construct Green's functions from E , $u(r)$, $v(r)$, and calculate the spin-spin correlation function $\chi(r; r^0; i_n)$ [23]. We obtain the nuclear spin relaxation rate,

$$\begin{aligned} R(r; r^0) &= \text{Im} \sum_n \chi(r; r^0; i_n) = (-T) \int \frac{dE}{2\pi} \\ &= \int \frac{dE}{2\pi} [u(r) u(r^0) v(r) v(r^0) \\ &\quad + v(r) u(r^0) u(r) v(r^0)] \\ &\quad T f^0(E) (E - E_0) \end{aligned} \quad (4)$$

with the Fermi distribution function $f(E)$. We consider the case $r = r^0$ by assuming that the nuclear relaxation occurs at a local site. Then, r -dependent relaxation time is given by $T_1(r) = 1/R(r; r)$. We use $\chi(x) = \frac{1}{i} \text{Im} \chi(x)$ to handle the discrete energy level of the finite size calculation. We typically use $\mu = 0.01t$. In Eq. (4), the first term is proportional to the $N_+(r; E) N_-(r; E)$ when $r = r^0$. To understand the behavior of $T_1(r)$, we also consider the LDOS given by $N(r; E) = N_+(r; E) + N_-(r; E) = \int \frac{dE}{2\pi} [u(r) u(r^0) f(E) + v(r) v(r^0) f(E + E_0)]$.

By solving Eq. (3) self-consistently, we obtain the order parameter Δ_{ij} and the sublattice magnetization M_i as shown in Fig. 1. It is seen that the moment is induced exclusively around the vortex core where the order parameter vanishes. The checkerboard modulation of M with eight site period along x and y directions is superimposed. This is barely seen in Fig. 1(b) where the "floor" in M is modulated with eight-site period. In the Fourier transformation of $S_{z,i}$ the eight-site period spin structure gives rise to peaks at the corresponding wave number Q in addition to the peak of the vortex lattice period. As U increases the checkerboard modulation with two ordering vectors $Q = (\frac{3}{4}; 0)$ and $(0; \frac{3}{4})$ changes into a one-dimensional stripe form characterized by $Q = (\frac{3}{4}; 0)$ or $(0; \frac{3}{4})$ (see Fig. 2 in Ref. [12] for stronger stripes). The induced moment at the core increases also with U . This spin modulation accompanies the charge modulation with $2Q$, namely, four site periodicity. The core accommodates excess particles, which is opposite to the stripe-free case where it does excess holes [26]. These results basically coincide with the previ-

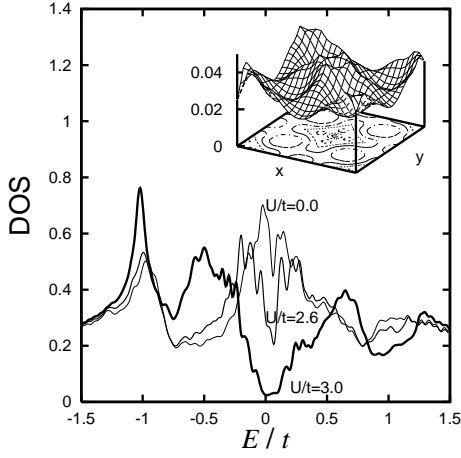


FIG. 2: Local density of states $N(r; E)$ at the core site for $U/t = 0; 2.6; 3.0$. The zero-energy state at $E = 0$ for $U/t = 0$ is gradually suppressed with U . Inset shows the spatial profile of the zero-energy LDOS $N(r; E = 0)$ for $U/t = 3.0$. $T/t = 0.01$.

ous studies [12, 13, 14, 15, 16] and also capture the essential features observed by STM experiment [4]. The vortex core changes to a circular shape by induced moment as seen from Fig. 1 (a). When $U = 0$ its shape was square like. [28]

In Fig. 2 we plot the LDOS as a function of the energy E/t at the core site. For the small $U/t = 2.6$ case where the appreciable moment is not induced, the ZEP appears, centered at $E/t = 0$. As U/t increases, the ZEP splits and is gradually suppressed. A gap-like feature becomes evident for $U/t = 3.0$ in Fig. 2. It is noted that the removed DOS at $E = 0$ piles up inside the bulk gap at $E/t = 1$. This DOS feature resembles the bound state at $E = 8\text{ meV}$ observed by STM on $\text{YBa}_2\text{Cu}_3\text{O}_{7-x}$ [7]. The inset shows the spatial distribution of the zero-energy state: When the induced moment is absent ($U = 0$), the zero-energy state accumulates at the core site. This is altered by introducing the induced moment, namely, $N(r; E = 0)$ decreases towards a core after taking a maximum. This is contrasted with the peak structure at a core in the stripe-free case (see Fig. 6 in Ref. [23]). We also note that the LDOS at $E = 0$ shown in inset contains the Fourier component with 4-site checkerboard modulation.

We depict the spatial distribution for $T_1^{-1}(r)$ at low T ($T/t = 0.01$) for $U/t = 3.0$ in upper panel of Fig. 3. It is seen that corresponding to the depressed LDOS at the core shown in Fig. 2 due to the induced moment, $T_1^{-1}(r)$ diminishes around the vortex core after it increases with approaching the vortex from far sites. In lower panel of Fig. 3, $T_1^{-1}(r)$ is depicted along the selected paths in the vortex lattice shown in upper panel. It is clearly seen that (1) $T_1^{-1}(r)$ at the core site V takes a local minimum. (2) One of the minima of $T_1^{-1}(r)$ occurs at C -point. (3) The relative $T_1^{-1}(r)$ values at V and C points depend on the magnitude of the induced moment. When J/t is large enough, $T_1^{-1}(r)$ becomes the absolute minimum at

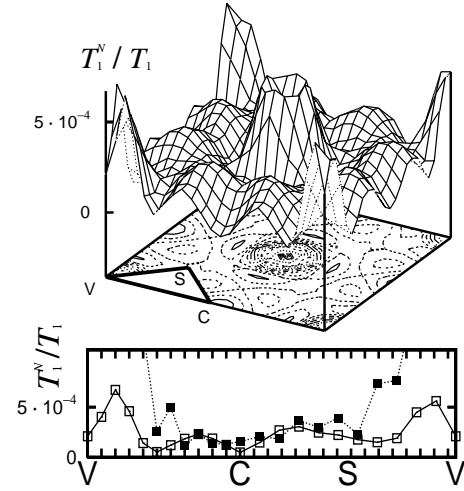


FIG. 3: Spatial profile of $T_1^{-1}(r)$ (upper panel). $T_1^{-1}(r)$ variation along the path (lower panel): $V \rightarrow C \rightarrow S \rightarrow V$ where empty (filled) squares correspond to $U/t = 3.0$ ($U/t = 0$). In the stripe-free case ($U/t = 0$) $T_1^{-1}(r)$ at V is extremely large. T_1^N is the normal state value at T_c .

V . (4) The maximum $T_1^{-1}(r)$ occurs near the core site whose distance from the core depends on J/t . In larger J/t case this distance becomes large because of the larger LDOS suppression due to the induced moment.

Both site-selective experiments of ^{17}O NMR on $\text{YBa}_2\text{Cu}_3\text{O}_{7-x}$ [5] and $\text{YBa}_2\text{Cu}_4\text{O}_8$ [6] for the CuO_2 planar site show that $T_1^{-1}(r)$ at the core is smaller than the neighboring sites for a certain H and T region. The $T_1^{-1}(r)$ maximum occurs in the vicinity of the core, i.e. $T_1^{-1}(r)$ decrease with increasing the internal field around the vortex core region. These facts are reproduced by our calculation, evidencing the usefulness of the site-selective NMR method in general. When we see the $T_1^{-1}(r)$ variation along $C \rightarrow S \rightarrow V$ in the experimental data [5, 6], $T_1^{-1}(r)$ has a minimum near the saddle point S . This behavior is also reproduced in our calculation of the stripe state here, while in the previous calculation ($U = 0$), $T_1^{-1}(r)$ monotonically increases along $C \rightarrow S \rightarrow V$ as displayed in lower panel in Fig. 3.

We show the T -dependence of $1/T_1(r)T$ for three sites in Fig. 4. It is seen that $1/T_1(r)T$ at the vortex site V displays a large enhancement around T_M below which M begins to appear as shown in the inset. Thus for $T_M < T < T_c$ the zero-energy state increases $1/T_1T$ and for $T < T_M$ the induced moment opens a gap at $E = 0$ as shown in Fig. 2, reducing $1/T_1T$ towards low T . The $1/T_1T$ behavior in the nearest neighbor site to the core is moderately enhanced at T_M while that in S -site remains same as in the stripe-free case. These correspond to the fact that the induced moment is limited only near the core. We should remark here that the enhancement in $1/T_1T$ below T_c delicately depends on applied field. As H increases, it is suppressed rather easily (see Fig. 12 in Ref. [23]).

The diverging behavior in $1/T_1(r)T$ at the core site

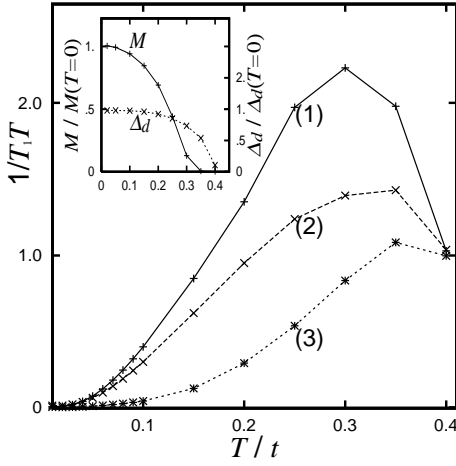


FIG. 4: T -dependence of $1/T_1 T$ for three sites. (1) The vortex core (V). (2) The nearest site to the core. (3) The saddle point site (S). Inset shows the corresponding T -dependence of Δ_d and M at their maximum values. $U=t=3.0$:

is strikingly similar to that observed in ^{205}Tl NMR on $\text{Tl}_2\text{Ba}_2\text{CuO}_6$ [20]. Our calculation is also consistent with $1/T_1 T$ behavior at the S point: Their data show strong decrease of $1/T_1 T$ at S below T_c and $1/T_1 T = \text{constant}$ at lower T , indicative of the zero-energy state.

As for Mitrovic's data [21], they observe that (A) $1/T_1 T$ inside the core is enhanced as lowering T while (B) $1/T_1 T$ outside the core stays at a constant which increases as H increases. These behaviors are understandable if we assume that T_M is low in $\text{YBa}_2\text{Cu}_3\text{O}_7$, namely their experiments are done for $T > T_M$: We can explain the fact (A) because as lowering T the thermal smearing factor coming from $f^0(E)$ in eq.(4) becomes narrow enough to see the sharp ZEP, driving $1/T_1 T$ to increase towards $T \rightarrow 0$. The fact (B) is consistent with the previous more detailed NMR at the saddle point by Zheng, et

al.[27] on $\text{YBa}_2\text{Cu}_4\text{O}_8$: They conclude that $1/T_1 T \propto H$ at the saddle point at low T . As shown previously the spatial average DOS $N(0) \propto H^{0.41}$ for d-wave case [28], then $1/T_1 T \propto N(0)^2 \propto H^{0.82}$, explaining the approximate H -linear behavior within the present experimental accuracy.

Many ordinary T_1 measurements are done by using the resonance field at the maximum intensity which corresponds to the saddle point S of the field distribution in the vortex state. Above T_c , $1/T_1 T$ shows a variety of different T -behaviors, depending on probed nuclei, such as O, Cu, Y, etc, or materials, or doping levels. These concern the so-called pseudo-gap phenomena. In contrast, the low T behaviors, remarkably enough, are quite similar, namely, a T^3 -law below T_c which is crossed over to the T -linear law at lowest T . The former T^3 -law indicates a line node for d-wave pair while the T -linear law is indicative of the zero-energy state outside of the vortex core, in spite of possible existence of the induced stripe. This is due to the fact that the induced moment is confined in the narrow core region and LDOS or T_1^{-1} is modified only there as seen from the lower panel of Fig.3.

In conclusion, we have calculated the site-dependent relaxation time $T_1^{-1}(r)$ for NMR, taking into account the possibility of the field-induced moment. The large $T_1^{-1}(r)$ enhancement observed in the vortex core site NMR in ^{205}Tl of $\text{Tl}_2\text{Ba}_2\text{CuO}_6$ is explained by our calculation. Other experiments for the vortex imaging [5, 6, 21] are also analyzed in a coherent manner. An emerging notion through these analyses, together with other STM and neutron scattering experiments, is the field-induced stripe picture in the vortex state of high T_c superconductors. The strength of the induced stripe depends on material's parameters. The existing data show that $\text{Tl}_2\text{Ba}_2\text{CuO}_6$ is strong while $\text{YBa}_2\text{Cu}_3\text{O}_7$ and $\text{YBa}_2\text{Cu}_4\text{O}_8$ are weak.

We thank K. Kumagai, Y. Matsuda and K. Ishida for useful discussions on their NMR.

-
- [1] B. Lake, et al., Nature 415, 299 (2002).
 - [2] S. Katano, et al., Phys. Rev. B 62, R14677 (2000).
 - [3] B. K. Haykovich, et al., Phys. Rev. B 66, 014528 (2002).
 - [4] J. E. Hoffman, et al., Science 295, 466 (2002).
 - [5] V. F. Mitrovic, et al., Nature 413, 501 (2001).
 - [6] K. Kakuyanagi, K. Kumagai, and Y. Matsuda, Phys. Rev. B 65, 60503 (2002).
 - [7] Ch. Renner, et al., Phys. Rev. Lett. 80, 149 (1998).
 - [8] H. F. Hess, et al., Phys. Rev. Lett. 62, 214 (1989) and Phys. Rev. Lett. 64, 2711 (1990).
 - [9] N. Hayashi, M. Ichioka, and K. Machida, Phys. Rev. Lett. 77, 4074 (1996).
 - [10] D. P. Arovas, A. J. Berlinsky, C. Kallin, and S. C. Zhang, Phys. Rev. Lett. 79, 2871 (1997).
 - [11] M. Ogata, J. Mod. Phys. B 13, 3560 (1999).
 - [12] M. Ichioka, M. Takigawa, and K. Machida, J. Phys. Soc. Jpn. 70, 33 (2001).
 - [13] E. Demler, S. Sachdev, and Y. Zhang, Phys. Rev. Lett. 87, 067202 (2001).
 - [14] J.-X. Zhu and C. S. Ting, Phys. Rev. Lett. 87, 147002 (2001).
 - [15] Y. Chen and C. S. Ting, Phys. Rev. B 65, 180513(R) (2002).
 - [16] J.-X. Zhu, I. Martin, and A. R. Bishop, Phys. Rev. Lett. 89, 067003 (2002).
 - [17] Per Hedegard, cond-mat/0102070.
 - [18] M. Ichioka and K. Machida, J. Phys. Soc. Jpn. 71, No.8 (2002).
 - [19] D. Podolsky, cond-mat/0204011.
 - [20] K. Kakuyanagi, K. Kumagai, Y. Matsuda, and M. Hasegawa, cond-mat/0206362.
 - [21] V. F. Mitrovic, et al., cond-mat/0202368.
 - [22] M. Takigawa, M. Ichioka, and K. Machida, Phys. Rev. Lett. 83, 3057 (1999).

- [23] M. Takigawa, M. Ichioka, and K. Machida, J. Phys. Soc. Jpn. 69, 3943 (2000).
- [24] D. K. Morr and R. W. Ortis, Phys. Rev. B 61, R 882 (2000).
- [25] T. Tohyama, S. Nagai, Y. Shibata, and S. Maekawa, Phys. Rev. Lett. 82 (1999) 4910.
- [26] N. Hayashi, M. Ichioka, and K. Machida, J. Phys. Soc. Jpn. 67, 3368 (1998).
- [27] G.-q. Zheng, et al., Phys. Rev. B 60, R 9947 (1999).
- [28] M. Ichioka, A. Hasegawa, and K. Machida, Phys. Rev. B 59, 184 (1999).